Mon. Not. R. Astron. Soc. **364,** 1429–1440 (2005) doi:10.1111/j.1365-2966.2005.09682.x

Radiative transfer effects on the Lyα forest

A. Maselli[1]★ and A. Ferrara[2]

[1]*Dipartimento di Astronomia, Universitá di Firenze, Largo Enrico Fermi 5, 50125 Firenze, Italy*
[2]*SISSA/International School for Advanced Studies, via Beirut 2-4, 34014 Trieste, Italy*

Accepted 2005 September 28. Received 2005 September 27; in original form 2005 May 10

ABSTRACT

Strong observational evidence for a fluctuating ultraviolet background (UVB) has been accumulating through a number of studies of the H I and He II Lyα forest as well as accurate intergalactic medium (IGM) metallicity measurements. UVB fluctuations could arise both from the inhomogeneous distribution of the ionizing sources and/or from radiative transfer (RT) through the filamentary IGM. In this study we investigate, via numerical simulations, the role of RT effects, such as shadowing, self-shielding and filtering of the ionizing radiation, in giving rise to a fluctuating UVB. We focus on possible detectable signatures of these effects on quantities derived from Lyα forest spectra, as photoionization rate fluctuations, $\eta(\equiv N_{\rm He\,II}/N_{\rm H\,I})$ parameter distributions and the IGM temperature at $z \approx 3$. We find that RT induces fluctuations up to 60 per cent in the UVB, which are tightly correlated to the density field. The UVB mean intensity is progressively suppressed toward higher densities and photon energies above 4 Ryd, due to the high He II opacity. Shielding of overdense regions ($\Delta \gtrsim 5$) from cosmic He II ionizing radiation produces a decreasing trend of η with overdensity. Furthermore, we find that the mean η value inferred from H I–He II Lyα forest observations can be explained only by properly accounting for the actual IGM opacity. We outline and discuss several implications of our findings.

Key words: radiative transfer – methods: numerical – cosmology: theory – diffuse radiation – large-scale structure of Universe.

1 INTRODUCTION

The lack of the Gunn–Peterson trough in the spectra of quasars at redshift $z < 5$ indicates that the intergalactic medium (IGM) after that epoch is photoionized by the ubiquitous presence of a metagalactic ionizing radiation, also known as the ultraviolet background (UVB).

Usually, studies of the so-called Lyα forest (the highly ionized absorbers that give rise to the absorption lines in quasar spectra) assume the UVB to be spatially uniform, with the same intensity and spectral shape everywhere in the Universe at a given redshift. This is a good approximation if the sources of the UVB radiation are uniformly distributed in space, as long as the attenuation volume is large enough to contain a fair sample of both the sources and the attenuating structures (Zuo 1992a). This last condition would imply a low cosmic optical depth, τ, to ionizing photons after reionization ($z < z_{\rm i}$). The cosmic optical depth should be low enough in fact, to ensure the attenuation length is larger than the typical separation between sources producing the UVB, which is $\lambda_{\rm s} \sim 100\,h^{-1}$ Mpc (comoving) for quasars and more than an order of magnitude less for galaxies. The relative contribution of these two populations to the UVB is unclear. Different independent studies have found that the contribution from galaxies should be at least comparable to that of quasars (Giallongo, Fontana & Madau 1997; Shull et al. 1999; Bianchi, Cristiani & Kim 2001; Kim, Cristiani & D'Odorico 2001; Steidel, Pettini & Adelberger 2001; Sokasian, Abel & Hernquist 2003) in the redshift range 2–3. As a caveat, we recall that Meiksin (2005) has pointed out that quasi-stellar objects (QSOs) might dominate the UVB in the redshift range $2 < z < 3$; according to his study QSO counts are highly uncertain near $z = 3$ and seem to be sufficient to account for the UVB at $z = 2$. The expected signature of a significant contribution from galaxies is a considerable softening of the UVB spectrum compared to previous models assuming quasars as the sole sources of ionizing radiation (Haardt & Madau 1996, hereafter HM96).

Although the IGM at $z < z_{\rm i}$ is highly ionized, cosmic mildly overdense regions, which give rise to the Lyα forest, contain enough neutral hydrogen and singly ionized helium to significantly attenuate the Lyman continuum flux from the sources of the UVB. As a result, the condition $\lambda_{\rm p} \gg \lambda_{\rm s}$ might not be fulfilled. For this reason, the metagalactic ionizing flux has been modelled starting from the intrinsic spectra of the ionizing sources, subsequently filtered through the IGM (HM96; Fardal, Giroux & Shull 1998). In

★E-mail: maselli@mpa-garching.mpg.de

brief, these calculations consist of reprocessing the UVB photons in a clumpy photoionized universe, by solving the radiative transfer (RT) equation in one dimension. The space density along the photon propagation direction and the physical properties of the sources (as well as of those of the absorbing clouds) are assumed as the average of the observed values, and the spectral redshift evolution of the UVB, assumed to be uniform in space, is derived.

Clustering of the ionizing sources and scattering in their emission properties, together with inhomogeneities in the IGM density field, can introduce significant fluctuations in both the intensity and spectral shape of the UVB.

Indeed, increasingly strong observational evidence for a significantly variable metagalactic ionizing radiation has been accumulating through a number of studies of the H I and He II Lyα forest. In a highly photoionized gas, the ratio of He II to H I column density, defined as the η parameter, is proportional to the ratio of H I to He II photoionization rates (Fardal et al. 1998): $\eta \equiv N_{\rm He\,II}/N_{\rm H\,I} \propto \Gamma_{\rm H\,I}/\Gamma_{\rm He\,II}$.

Kriss et al. (2001) and Shull et al. (2004) analysed the *Far-Ultraviolet Spectroscopic Explorer* (*FUSE*) observations of the fluctuating He II absorption toward the bright quasar HE 2347−4342 at $z = 2.885$. Using H I Lyα data from Keck and the High-Resolution Echelle Spectrograph (HIRES), they found an H I counterpart for more than 50 per cent of the He II absorption lines. The measured η values cover a wide range from 1 to 1000 (with an average $\langle\eta\rangle \approx 80$). Analogous observations of the He II Lyα forest towards HS 1700+6416, by Reimers et al. (2004), reveal a similar η variation. The large scatter is a clear signature from an ionizing background which is significantly fluctuating throughout the IGM. Shull et al. (2004) pointed out two important points: (i) a small-scale η variability (on typical scales of $\Delta z \sim 10^{-3}$, corresponding to about $1\,h^{-1}$ Mpc comoving at $z \sim 3$); (ii) an observed correlation of high-η (i.e. soft ionizing spectra) absorbers with low-density regions (voids in the H I Lyα distribution). The authors further suggest that these effects, confirmed by the Reimers et al. (2004) observations, might be caused either by spatial/spectral fluctuations of the ionizing sources on scales of 1 Mpc, or by RT effects through a filamentary IGM whose opacity variations control the penetration of 1–5 Ryd radiation over 30–40 Mpc distances (a combination of the two is also possible).

Although recent *Hubble Space Telescope* (*HST*) observations (Telfer et al. 2002) show a broad distribution of QSO spectral indices from $\alpha \simeq 0$ to 3 ($J_\nu \propto \nu^{-\alpha}$ representing the quasar spectrum) this spread could hardly be advocated to explain the small-scale η fluctuations. The reason is that the QSO mean separation ($\approx$100 Mpc comoving at $z \sim 3$) exceeds by far the characteristic scale of about $1\,h^{-1}$ Mpc on which the η variations are observed. RT through an inhomogeneous medium appears to be the most natural origin for such fluctuations. In turn, these might result from a number of effects, such as shadowing, self-shielding and filtering of the radiation. All these effects act on the same scales of the inhomogeneities in the IGM, thus on scales smaller than 1 Mpc. It is then important to study the correlation function of both J_ν and η with the density fluctuations.

Nakamoto, Umemura & Susa (2001) were the first to attempt to account for the RT effects of a background ionizing radiation. They focused on the reionization of an inhomogeneous universe, looking at the evolving configuration of the neutral hydrogen distribution, but not directly at the fluctuations in the radiation field. None the less, emphasizing the deviations of the neutral hydrogen distribution obtained in their simulation from the case of a perfectly transparent medium embedded in a uniform ionizing background, they indirectly stressed the importance of RT effects such as self-shielding and shadowing by translucent regions, which indeed have been well reproduced by their simulations.

RT is furthermore expected to have some effect on the IGM temperature. Previous studies (Abel & Haehnelt 1999; Bolton, Meiksin & White 2004) focused on the effects of RT on the temperature evolution during reionization, i.e. behind an ionization-front (I-front) expanding in a neutral or mildly ionized IGM. These analyses have shown that RT can boost the mean gas temperature with respect to the case in which an instantaneous, uniform reionization occurs [i.e. its optically thin (OT) counterpart], as a consequence of filtering effects. In fact, the ionizing spectrum across the I-front becomes harder as it expands further from the ionizing source, because most of the low-energy photons (having higher cross-sections) are absorbed by recombining atoms inside the H II region, and its photoheating power increases accordingly. The overall predicted RT effects are: (i) an enhancement of the IGM temperature by a factor of $\approx$2 after reionization; (ii) increased scattering in the temperature–density relation; (iii) a strong hardening of the metagalactic ionizing flux after the He II reionization. Here we consider the more stationary situation in which the mean ionization level in the simulation volume remains roughly constant; hence, strong RT signatures on the IGM temperature are not expected. Nevertheless, we look for a systematic dependence of the photoheating rates on the density.

So far, much of the work in studying UVB fluctuations has been done to assess the effects produced by the inhomogeneous distribution of ionizing sources, almost neglecting or just approximately including the effects of RT through the filamentary IGM. Zuo (1992a,b) first developed a theory to deal with the fluctuations produced by randomly distributed ionizing sources, in terms of the probability distribution of the ionizing UV radiation field (Zuo 1992a) and of its two-point correlation function (Zuo 1992b). Meiksin & White (2003) made a step forward by applying Zuo's formalism to the ionizing source distribution derived via numerical simulations of structure formation. A few groups have studied, through numerical simulations, the effects on the statistical properties of the Lyα forest of UVB fluctuations induced by source clustering or non-uniform emissivity properties as light-cone effects, QSO time variability, lifetime and spectral index scattering. Gnedin & Hamilton (2002) first investigated via RT simulations the effects of UVB fluctuations induced by the quasar inhomogeneous distribution, on the matter power spectrum inferred from the observed/simulated transmissivity of the Lyα forest (Croft et al. 1999). By comparing the mock spectra from RT simulations and from simulations assuming photoionization equilibrium with a uniform UVB, they found the effects of RT to be negligible for the power spectrum; nevertheless, it is interesting to notice that, in order to match the observed transparency of the IGM, the mean photoionization rate required when including properly RT, has to exceed by 20 per cent that required in the OT approximation. Meiksin & White (2004) attempted to quantify the UVB fluctuations and examined the possible effects on the power spectrum and autocorrelation function of the Lyα forest. They calculated the UVB intensity smearing out the radiation emitted from a discrete distribution of QSOs in the simulated volume, within an attenuation length whose evolution with redshift is evaluated modelling the gas density distribution with a particle mesh (PM) simulation. Their calculation separately adds the contribution of the Lyman limit system (LLS), which is not resolved in numerical simulations, on the basis of their observed statistical properties. Croft (2004) uses a time-independent ray tracing algorithm to model the space density of ionizing radiation produced by QSOs at $z \approx 3$, neglecting its feedback on the ionization state of the IGM.

The study is based on N-body simulations and prescriptions must be used to relate the dark matter density and the H I optical depth. McDonald et al. (2005) use a rough self-shielding approximation, in which the background radiation in each cell is attenuated by the column density of that cell; shadowing and filtering effects are neglected altogether. The most relevant outcome of these studies for the present study is that UVB fluctuations induced by the discreteness of the UVB sources could be only relevant at high redshifts and on large scales. Below $z = 4$, the importance of such fluctuations rapidly decreases, as a consequence of the increase of $\lambda_{\rm p}$ which smoothes the flux at a given position over a larger ensemble of sources.

For this reason, we take here a complementary, and still unexplored, approach which consists of the investigation of UVB fluctuations introduced by the RT effects mentioned above. We focus on possible detectable signatures of these effects on quantities derived from Lyα forest spectra, as photoionization rate fluctuations, the temperature–density relation and η parameter distributions. To this aim we have performed RT simulations, applying CRASH (Maselli, Ferrara & Ciardi 2003, hereafter MFC03) to a cosmological density field exposed to an ionizing background radiation characterized by a spatially constant emissivity. Such a radiation field, by interacting with the filaments of the cosmic web, is rapidly turned into a fluctuating one. The rest of the paper is devoted to study and quantify this effect.

2 NUMERICAL SIMULATIONS

The aim of the present study is to estimate the effects of RT on the metagalactic ionizing radiation and the resulting effects induced in the physical properties of the IGM. The present study is focused at $z \approx 3$. We have exposed a snapshot at a fixed redshift of a cosmological density field to an (initially) uniform ionizing radiation field. The density field has been derived with the numerical code described in Marri & White (2003), a modified, multiphase version of the entropy-conserving smoothed particle hydrodynamics (SPH) code GADGET2 (Springel, Yoshida & White 2001). Several algorithms have been designed to reduce artefacts which occur in cold, dense gas clouds embedded in a hot diffuse halo; the code includes a new implementation of feedback which allows supernova energy to be channelled effectively into the heating of diffuse gas and the evaporation of cold clouds. A multiphase description of the interstellar medium is adopted, based on an explicit separation of protogalactic gas into diffuse and dense (star-forming) components, which is able to suppress star formation, reheat cold gas and drive outflows from galactic discs. The presence of a UV background produced by QSOs is included in the OT approximation following HM96 from which the IGM temperature and ionization state are calculated assuming photoionization equilibrium.

We use here a snapshot at $z = 3.27$ from a simulation which has been used and analysed in previous works of our group (Bruscoli et al. 2003; MFC03; Fangano, Ferrara & Richter, in preparation). These studies have shown that the statistical properties of the IGM, e.g. the probability distribution function (PDF) of the transmitted Lyα flux, are correctly reproduced. The simulation uses 128^3 particles in a $10.5\,h^{-1}$ comoving Mpc box (corresponding to a mass resolution of 8.5×10^6 $M_\odot$ in gas) and assumes a Λ cold dark matter (CDM) cosmological model with $\Omega_0 = 0.3$, $\Omega_\Lambda = 0.7$, $\Omega_{\rm b} = 0.04$, $h = 0.7$ and $\sigma_8 = 0.9$; periodic boundary conditions are assumed.

2.1 Radiative transfer

We have performed the RT calculation using the code CRASH. A detailed description of the code, its performances and several test problems can be found in MFC03, to which we refer the interested reader. In the present study we neglect the effects of cosmological expansion; this choice is motivated by the fact that the light crossing time of an attenuation length ($\sim$100 Mpc) is roughly one-tenth of the Hubble time at the redshift of interest. We have exposed the density field obtained from the SPH simulation to a UVB radiation with spatially constant emissivity. The UVB is subsequently modified as it propagates in the filamentary density field by self-shielding, shadowing and spectral filtering effects, finally resulting in a fluctuating field. The RT simulation has been evolved for a physical time, $t_{\rm s} = 0.7 \times 10^7$ yr. This choice has been made, after some experiments, to guarantee that numerical convergence of the solution is achieved. It has to be noticed that here the simulation time does not correspond to a physical evolution of the background, but it is the time required for the gas ionization and temperature to reach equilibrium in the self-consistently radiation field shaped by RT. In the following we discuss two crucial, albeit somewhat technical, points concerning a new implementation of a uniform radiation background in CRASH and its flux calibration within the simulation.

2.1.1 Simulating a uniform ultraviolet background

The algorithm described in MFC03 for the implementation of the presence of a uniform background radiation in the simulation box has been improved in several ways. In the original implementation, background radiation was modelled by allowing box boundary cells to emit photons packets with the prescribed UVB spectral energy distribution. Although this choice is suitable for some types of problems, it cannot match the high accuracy required by the present study. To better fulfil such a requirement we have devised a new implementation in which all cells in the box, but those with overdensity $\Delta = \rho/\langle\rho\rangle \leqslant \Delta_{\rm e}$, behave as UVB radiation sources, in the sense that they emit photon packets.[1] The threshold on the overdensity is meant to preserve the effect of self-shielding in high-density regions and galactic haloes. For definiteness, we take the value corresponding to the typical overdensity of collapsed haloes at the virial radius. The exact value of $\Delta_{\rm e}$ depends on the density profile of the halo; it can be shown that it is $\approx$59.2 for a isothermal profile and it is $\approx$63.7 for the NFW profile (Navarro, Frenk & White 1996). In this paper, $\Delta_{\rm e} = 60$ has been assumed. We adopt periodic boundary conditions, so that packets can travel trough the simulation box for a number of cycles, $N_{\rm cyc}$, given by the ratio between the mean free path of ionizing photons, $\lambda_{\rm p}$, and the physical size, L, of the simulated volume. We have derived an estimate for $\lambda_{\rm p}$, running a benchmark simulation aimed at evaluating the statistical distribution of the mean free paths of photons – whose frequencies are distributed according to the HM96 spectrum – in the assigned density field. For this purpose, in the benchmark simulation we just follow the propagation of photons packets, i.e. not considering their effect on the gas properties; due to the statistical treatment of the packet energy deposition inherent to the Monte Carlo scheme (see Maselli et al. 2004), we define as 'absorbed' a packet whose initial energy has

[1] It is important to notice that here the cells emitting photons are not meant to reproduce physical sources of UV radiation; the adopted method aims at reproducing a uniform UVB in the simulated volume, within a Monte Carlo ray tracing scheme.

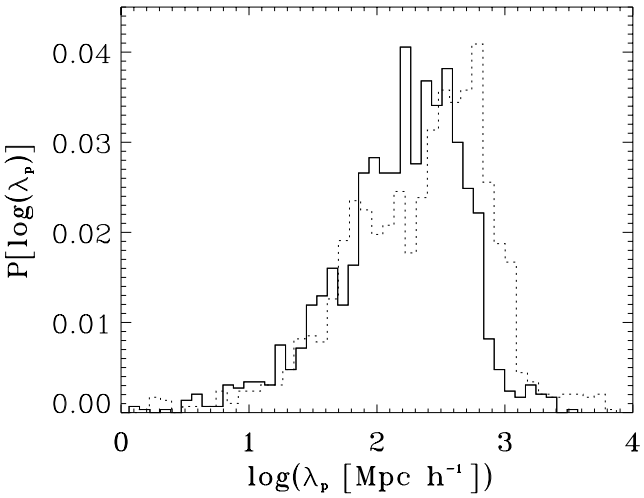

Figure 1. Distribution of the comoving mean free path of ionizing photons at $z = 3.27$ as derived from the SPH simulation. The solid curve includes opacity of both H I and He II; the dotted curve is for H I only.

been depleted by >95 per cent. In Fig. 1 we show the mean free path distribution obtained from such a numerical experiment. The solid curve corresponds to the mean free path obtained by including the opacity of both hydrogen and helium absorbers, whereas the dotted curve corresponds to H I opacity only. The mean (median) values of the two distributions are 300 and 495 h^{-1} Mpc (199 and 306 h^{-1} Mpc) comoving. This shows that the He II contribution to the diffuse IGM opacity is significant. The above value of λ_p, for H I opacity, is consistent with that inferred from Fan et al. (2002), $\lambda_p \approx 100\,h^{-1}$ Mpc at $z \approx 3$, by comparing observations of high-resolution quasar spectra with semi-analytical models of the Lyα forest with a simple schematic model of the IGM opacity based on a peak statistics approach.

Guided by this finding, and given our box size, we fix $N_{\rm cyc} = 10$. The agreement of the simulated and observed mean values of λ_p further supports the $N_{\rm cyc}$ choice above. Periodic boundary conditions allow us to simulate volumes smaller than the mean free path of neutral hydrogen ionizing photons, having thus a higher spatial resolution, without much information loss. However, we make clear that the main aim of the present study is RT effects on scales of ≈1 Mpc, the characteristic scale of IGM filaments; no attempt is made to describe large-scale fluctuations induced by non-uniform distribution of the UVB sources.

According to the CRASH Monte Carlo algorithm tracking photon packet propagation, the mean number of crossing events per cell is given by

$$\langle \mathcal{N}_{\rm cross} \rangle = \frac{N_{\rm cyc} N_{\rm p}}{N_{\rm c}^2} \qquad (1)$$

where $N_{\rm p}$ is the total number of photon packets in a single run and $N_{\rm c}^3$ is the number of grid cells in the computational volume.[2] The new background implementation has been tested by running a simulation in which we force the condition $\tau = 0$. Although, when not including cosmological expansion, the $\tau = 0$ assumption would imply an infinite radiation field (i.e. the Olber paradox), we get around this problem by fixing $N_{\rm cyc}$ to a finite value. All the parameters are then set in order to reproduce the required UVB intensity, as described in Section 2.1.1 Ideally, in this case the intensity of the UVB should be perfectly uniform, as fluctuations caused by photon–matter interactions (absorption and scattering), redistributing the ionizing radiation in space and frequency, are suppressed. In practice, uniformity can be achieved only up to a certain accuracy level, due to finite number packet statistics, which produces noise fluctuations in the emission pattern. The amplitude of such fluctuations decreases with increasing $N_{\rm p}$, which is however constrained by computational expense. We have performed different test runs increasing $N_{\rm p}$ to accurately quantify the amplitude of such fluctuations. Table 1 shows the computed rms of the fluctuations, σ_N, around the mean value of the UVB intensity as a function of the numerical parameters of the run. The values for $N_{\rm c}$ and $N_{\rm cyc}$ are the same adopted for the actual cosmological simulations.[3] These fluctuations are due to the photon shot noise intrinsic to the adopted numerical algorithm.

Table 1. Parameters of the simulation test runs used to check uniformity and calibration of the radiation field.

A	$N_{\rm p}$	$N_{\rm cyc}$	$N_{\rm c}$	$t_{\rm s}$ (yr)	σ_N
		Uniformity tests			
–	3×10^5	10	128	–	20 per cent
–	3×10^6	10	128	–	10 per cent
–	3×10^7	10	128	–	4 per cent
–	3×10^8	10	128	–	1 per cent
		Calibration tests			
0.95×10^{52}	10^6	10	32	10^5	1 per cent
0.95×10^{52}	10^6	5	32	10^6	10 per cent
0.95×10^{52}	10^7	10	64	10^7	3 per cent
0.95×10^{52}	3×10^8	10	128	10^7	2 per cent

From Table 1, we see that runs at higher resolution (i.e. higher values of $N_{\rm p}$) are characterized by a small intrinsic scatter of the radiation intensity: σ_N decreases from 20 per cent for $N_{\rm p} = 3 \times 10^5$, to less than 1 per cent for $N_{\rm p} = 3 \times 10^8$. At the same time, we have also checked that during these test runs $\langle \mathcal{N}_{\rm cross} \rangle$ closely matches the theoretical value (as expressed in equation 1). As a good compromise between accuracy and computational time we adopt $N_{\rm p} = 3 \times 10^7$ for the cosmological RT simulations. This value, according to the above tests, guarantees that the ionizing radiation field fluctuations are uniformly distributed within a precision level of 4 per cent. Hence, larger fluctuations seen in the simulation outputs can be safely attributed to RT effects.

2.1.2 Ultraviolet background intensity calibration

Particular attention must be devoted to the ionizing flux calibration. The problem arises when the emissivity has to be related to the photon content of packets originating from a cell, as it is not obvious how to convert the latter into the specific flux units in which J_ν is usually assigned (erg s^{-1} cm^{-2} Hz^{-1} sr^{-1}). To overcome the problem we have devised a calibration technique, which turns out to be highly precise and straightforward.

Given a set of simulation parameters, $N_{\rm p}$, $N_{\rm cyc}$, $N_{\rm c}$ and $t_{\rm s}$, the intensity of the radiation field can be tuned by varying the number

[2] In the OT case, a single packet crosses typically $N_{\rm cyc} N_{\rm c}$ cells, and thus the total number of crossings in a simulation is $N_{\rm p} N_{\rm cyc} N_{\rm c}$ for $N_{\rm c}^3$ cells (for more details, see MFC03).

[3] The intrinsic scatter σ_N, associated with the numerical resolution of a given run, does not depend on the physical time of the simulation, $t_{\rm s}$, and on the intensity of the UVB, which, as discussed later, depends on the normalization factor A.

of (monochromatic) photons contained in a packet, N_γ, at emission. We express this quantity as follows

$$N_\gamma = A\Delta t \frac{J(\nu)}{J_{912}} = A\frac{N_c^2 t_s}{N_p N_{cyc}} \frac{J(\nu)}{J_{912}} \quad (2)$$

where A is the calibration factor[4] to be determined and Δt is the mean time interval between two subsequent crossings of a cell by photon packets (for the second equality, see MFC03). A nice feature of the previous expression is its scaling with the simulation parameters. Once the intensity and the UVB spectral shape are fixed, the factor A is the same for any combination of the numerical parameters. An order of magnitude for A can be derived by equating the theoretical and numerical estimates of the ionization fraction increment, $\Delta x_{\rm H\,II}$, for a cell during the time interval Δt. We consider here, for the sake of clarity, the case of a pure hydrogen gas and a monochromatic spectrum $[J(\nu)/J_{912} = 1]$. The theoretical value is given by

$$\Delta x^t_{\rm H\,II} = \Gamma_{\rm H\,I} x_{\rm H\,I} \Delta t; \quad (3)$$

similarly, the numerical value can be expressed as

$$\Delta x^n_{\rm H\,II} = N_\gamma (1 - {\rm e}^{-\tau_c})/N_{\rm H\,I} = A\Delta t \tau_c / N_{\rm H\,I} \quad (4)$$

where τ_c is the cell optical depth, and $N_{\rm H\,I} = n_{\rm H\,I}\Delta x^3$, with Δx^3 being the cell volume, is the total number of H atoms in the cell; the last equality holds for the OT case ($\tau_c \ll 1$). By equating the two expressions, we can write A as

$$A = \frac{\Gamma_{\rm H\,I}}{\sigma_0}\Delta x^2, \quad (5)$$

where we have used $\tau_c \approx n_{\rm H\,I}\sigma_0\Delta x$, with σ_0 being the H I photoionization cross-section at the Lyman limit. For the RT simulations used in this study, $\Delta x \simeq 27$ kpc; hence, for a typical $\Gamma_{\rm H\,I} = 10^{-12}$ s^{-1}, $A \approx 10^{51}$ s^{-1}.

The determination of the exact value of A for the general case of a H/He gas and of a non-monochromatic spectrum is not as straightforward. The adopted strategy has been to select a cell at the centre of the simulation box, to assign it physical properties characteristic of the hydrodynamic simulation (we choose $n = 10^{-5}$ cm^{-3}, $T = 10^4$ K, $x_{\rm H\,I}$ the value at the photoionization equilibrium with the assigned $\Gamma_{\rm H\,I}$ value). We assume $\tau = 0$ for all remaining cells in the box; this guarantees that the ionizing radiation field impinging on the target cell has not been modified in either intensity or spectral shape by RT effects. In the above configuration, we run CRASH to compute the H I fraction in the central cell and the average photoionization rate, $\Gamma_{\rm H\,I}$, by counting the cumulative number of ionizing photons absorbed in a given simulation time. We then tune the value of A by requiring that the $x_{\rm H\,I}$ and $\Gamma_{\rm H\,I}$ estimated values match the assigned values within an accuracy of 1 per cent. We find that $\Gamma_{\rm H\,I} = 1.2 \times 10^{-12}$ s^{-1} (HM96) corresponds to $A = 1.55 \times 10^{52}$ s^{-1}.

As discussed above, the same value of A reproduces correctly the assigned ionization rate (for a given UVB spectral shape) independently of the values of N_p, N_{cyc}, N_c and t_s, provided that N_γ is evaluated according to equation (2). The degree of accuracy is shown in the bottom part of Table 1 where the rms deviation, σ_N, of the distribution of $\Delta x^n_{\rm H\,II}$ with respect to the theoretical value $\Delta x^t_{\rm H\,II}$ is shown for different combinations of the numerical parameters. The scatter is always less than 10 per cent, depending on the resolution of the run. The calibration method adopted results thus to be accurate and stable.

In actual RT simulations, we should further account for the opacity of the IGM in order to reproduce at each cell the correct ionizing flux;[5] the photon content of packets is in fact depleted while it propagates through the box, due to non-zero opacity of the IGM distribution. To counteract this effect, we boost the normalization parameter A by 2.3; the exact value of this factor has been determined empirically, requiring that the mean opacity of the simulated volume is the same for the OT (zero-opacity) and RT cases. If the calibration factors for the RT and OT cases are related according to the equation $A^{\rm OT} = A^{\rm RT}{\rm e}^{-\tau_{\rm eff}}$, it corresponds to an effective optical depth $\tau_{\rm eff} \approx 0.8$.

Extracting the correct physical values of the photoionization and photoheating rates (at each cell) from the RT simulation is also not straightforward. Again, we need a reference OT simulation (with the same numerical parameters) in order to calibrate correctly these values. The OT and RT simulations differ (i) in the normalization factor, $A^{\rm OT}$ and $A^{\rm RT}$ related as above, and (ii) in the fact that for the OT we do not allow for absorption to occur. In both RT and OT cases, summing up the contribution given at each crossing event, the following relations hold:

$$\Gamma_i = C_i \sum_{j\in{\rm cross}} N_\gamma(\nu_j)\sigma_i(\nu_j), \quad (6)$$

$$\mathcal{H}_i = C'_i \sum_{j\in{\rm cross}} N_\gamma(\nu_j)\sigma_i(\nu_j)(\nu_j - \nu_{{\rm th},i}).$$

Here j is the index counting the crossing events in a given cell and ν_j is the frequency of the packet at the jth crossing; C_i and C'_i are scaling factors which depend only on the numerical parameters and are the same for both the OT and RT cases. The other symbols follow the conventional notation. Having determined $A^{\rm OT}$ as seen above, we can safely impose that $\langle\Gamma_i^{\rm OT}\rangle = \Gamma_i^{\rm th}$ (e.g. $\Gamma_{\rm H}^{\rm OT} = 1.2 \times 10^{-12}$ s^{-1}) and accordingly derive C, which in turn is used to derive the correct $\Gamma_i^{\rm RT}$ physical values at each cell in the box.

Finally, we mention that in the RT simulation the emission of diffuse radiation from recombining gas (estimated to account for about 30 per cent of the ionizing background at $z = 3$) has been turned off inside CRASH. This is done to prevent double-counting of such radiation, which is already included in the HM96 computation of the adopted UVB.

3 RESULTS

In this section we present the results of the RT simulations. We first analyse the amplitude of RT-induced fluctuations as traced by UVB photoionization and photoheating rates of the three absorbers H I, He I and He II. These are defined as

$$\delta\Gamma_i = \frac{\Gamma_i - \langle\Gamma_i\rangle}{\langle\Gamma_i\rangle}, \qquad \delta\mathcal{H}_i = \frac{\mathcal{H}_i - \langle\mathcal{H}_i\rangle}{\langle\mathcal{H}_i\rangle}; \quad (7)$$

the index $i \in \{{\rm H\,I}, {\rm He\,I}, {\rm He\,II}\}$ denotes the absorbing species and the averages are performed over all the cells at the end of the RT simulation. We then focus on the effects of such fluctuations on the IGM $\eta \equiv N_{\rm He\,II}/N_{\rm H\,I}$ distribution, the η–density relation and on the IGM temperature–density relation, with the aim of identifying possible detectable signatures.

[4] Note that the calibration factor A has physical dimensions s^{-1}, i.e. a photoionization rate.

[5] By 'correct' we mean the ionizing flux which reproduces the assigned mean opacity.

3.1 Ultraviolet background fluctuations

Spatial fluctuations of the H I and He II photoionization rates are shown in Fig. 2 on a slice across the RT simulation box of (physical) depth $\Delta x \approx 27$ kpc, corresponding to one grid cell ($\delta\Gamma_{\rm H\,I}$ and $\delta\Gamma_{\rm He\,II}$ in the left and right panels, respectively). RT effects result in significantly fluctuating photoionization rates on scales of few comoving Mpc, whose structure is closely linked to the underlying density fluctuations. As shown in the following, typically regions of low overdensity (say $\Delta \lesssim 1$, often referred to as voids) have $\delta\Gamma > 0$, whereas overdense regions tend to have negative fluctuations. Comparing the two maps we can also notice that $\Gamma_{\rm He\,II}$ fluctuations are much stronger than those of $\Gamma_{\rm H\,I}$. In general, though, RT induces fluctuations of several tens of per cent of the mean ionizing flux in both species. Such deviations from a homogeneous radiation field are produced by the combined action of shielding and shadowing effects. Although these features can be qualitatively understood from simple physical arguments, their quantitative evaluation can only be carried out through full three-dimensional RT simulations.

In order to make the above statements more quantitative, we show in Fig. 3 the $\delta\Gamma_{\rm H\,I}$ and $\delta\Gamma_{\rm He\,II}$ distributions as a function of the local overdensity, Δ. Each point in the plots corresponds to a cell of the simulated grid. The plot in the left panel shows clearly how the mean amplitude of H I photoionization rate fluctuations varies with overdensity, passing from positive values (of the order of a few per cent) in the voids to negative values, larger than 10 per cent, towards higher densities. $\delta\Gamma_{\rm He\,II}$, shown in the right panel, exhibits an analogous trend, although with larger excursion, with values $\approx +25$ per cent (≈ -50 per cent) at the lowest (highest) density boundaries of the density range. Deviations from the mean value can be as high as 20 and 60 per cent, for $\Gamma_{\rm H\,I}$ and $\Gamma_{\rm He\,II}$ respectively, in structures corresponding to overdensities with $\Delta \gtrsim 50$, where therefore the UVB intensity appears to be significantly suppressed. The steeper dependence and larger scatter of the $\delta\Gamma_{\rm He\,II}$–$\Delta$ relation reflect the fact that the Universe is more opaque in He II than in H I. Note also that in underdense regions $\Gamma_{\rm He\,II}$ can exceed by more than 40 per cent the volume averaged mean value, $\langle\Gamma_{\rm He\,II}\rangle$.

We focus now on mildly overdense regions, such as filaments, which give rise to absorption lines in the Lyα forest. These regions are exposed to roughly the mean photoionization rates for H I, but the photoionization of He II is here suppressed by about 20 per cent with respect to the mean value. This fact suggests that the He III fraction,

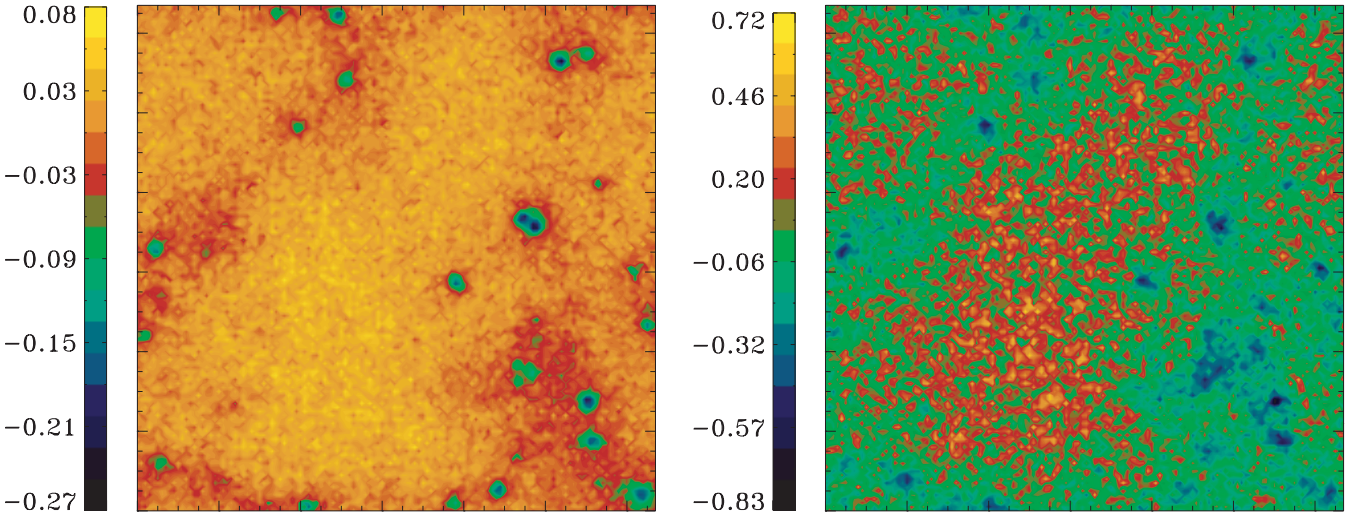

Figure 2. Spatial fluctuations of H I (left panel) and He II (right panel) photoionization rates in a slice across the RT simulation of (physical) depth $\Delta x \approx 27$ kpc. The curves denote the mean values.

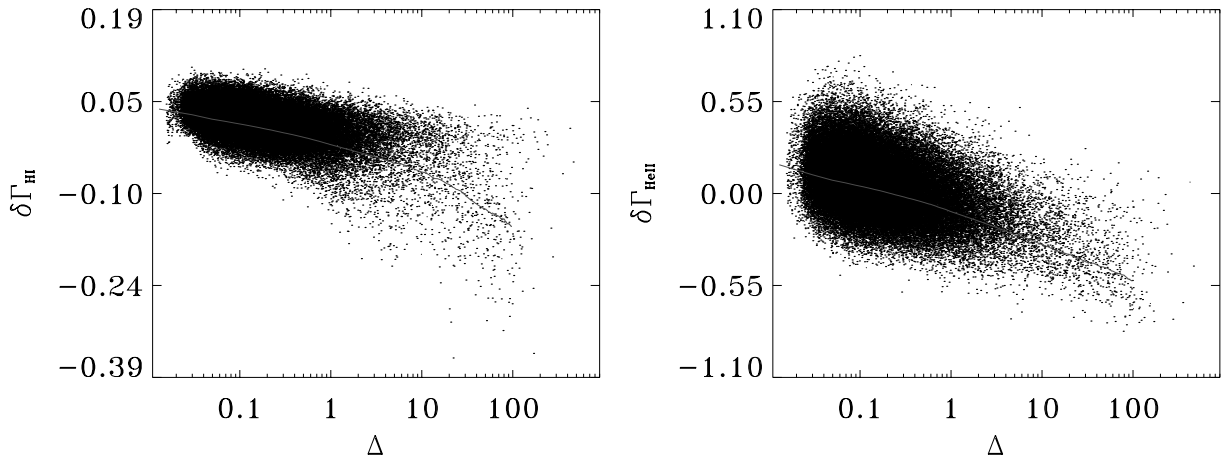

Figure 3. Spatial fluctuations of H I (left panel) and He II (right panel) photoionization rates, as a function of the local overdensity, Δ. Each point in the figures corresponds to a cell of the simulated grid; the solid lines show the mean $\delta\Gamma$ value as a function of Δ.

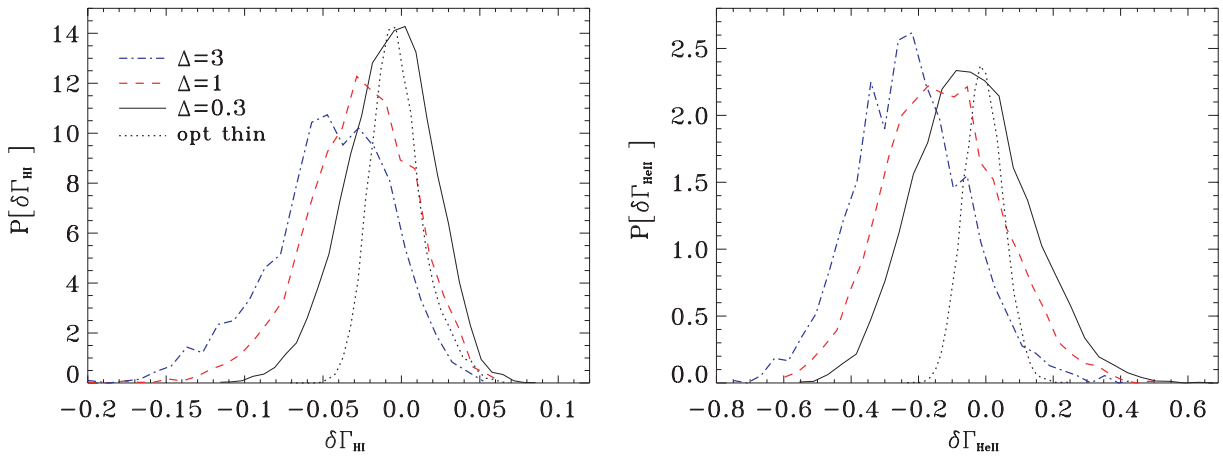

Figure 4. PDF of the fluctuations for three selected values of the overdensity, $\Delta = 0.3$ (solid line), $\Delta = 1$ (dashed line) and $\Delta = 3$ (dot-dashed line). The left and right panels refer to $\delta\Gamma_{\rm H\,I}(\Delta)$ and $\delta\Gamma_{\rm He\,II}(\Delta)$, respectively. The dotted curves are the analogous distributions at $\Delta = 0.3$ for the OT case.

which in both numerical simulations and data interpretation of Lyα forest is usually derived assuming photoionization equilibrium with a uniform UVB, is probably seriously overestimated. The ultimate physical nature of the decreasing trend of $\delta\Gamma_i$, with $i \in \{\rm H\,I, He\,II\}$, with density is a mixture of self-shielding and shadowing effects.

It is very instructive to inspect the PDF of the fluctuations at fixed overdensities. Fig. 4 shows such a distribution at $\Delta \in \{0.3, 1, 3\}$ (solid, dashed and dot-dashed curves, respectively), for $\delta\Gamma_{\rm H\,I}(\Delta)$ (left panel) and $\delta\Gamma_{\rm He\,II}(\Delta)$ (right panel). The distributions resemble Gaussian curves whose mean value decreases with Δ. The shift of the mean is caused by the increasing importance of the shielding and it is about five times larger for He II ($= -0.25$) than for H I ($= -0.05$): as explained above, the attenuation of the flux due to the structure shielding is more prominent above 4 Ryd due to the larger opacity at those energies. In the case of H I, a significant increase of the distribution width is observed towards larger overdensities; in contrast, the three distributions obtained for $\delta\Gamma_{\rm He\,II}$ show a similar dispersion. This results from the fact that, while the H I optical depth of the IGM is dominated by rare, overdense regions, the He II optical depth is non-negligible even in voids. This fact is confirmed if we look at the probability distribution for the mean free path of photons at 1 and 4 Ryd, shown in Fig. 5 (solid and dot-dashed curves, respectively). For 1-Ryd photons, the mean free path distribution is highly peaked at roughly $60\,h^{-1}$ Mpc,[6] showing that these photons are preferentially absorbed in high-density peaks. The 4-Ryd photon mean free path distribution is wider and has a mean value of about $7\,h^{-1}$ Mpc, which is a clear indication for a significant contribution of voids to the He II opacity.

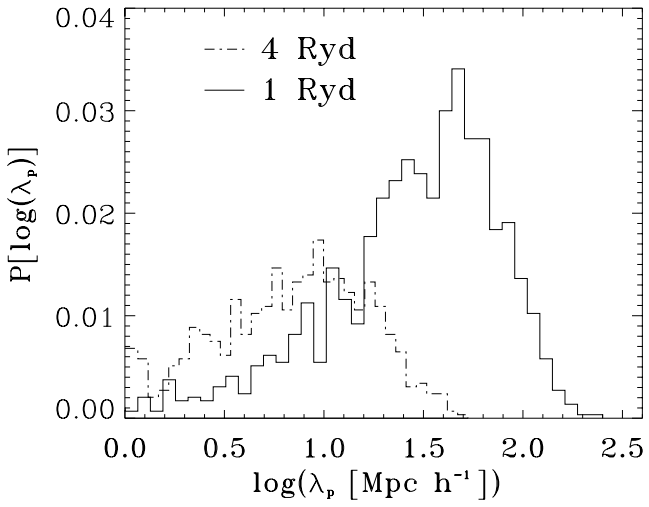

Figure 5. Probability distribution of the mean free path of photons at 1 Ryd (solid curve) and 4 Ryd (dot-dashed curve).

We have checked that the dispersion of the flux distribution shown in Fig. 4 does not result from spurious effects introduced by the emission algorithm, comparing the distributions above with the analogous distributions derived in the OT simulation.[7] The latter are shown in the panels of Fig. 4 by the dotted curves for $\Delta = 0.3$ (as the OT distribution does not depend on overdensity, we only plot this case). For visualization purposes, these curves have been normalized so that their peaks match the peaks of the corresponding RT distributions. The dispersion of these distributions is obviously unphysical as it represents the intrinsic error of the numerical algorithm, which is of the order of 4 per cent for H I, as already pointed out in Table 1, and more than twice for He II (∼10 per cent); the higher numerical dispersion for He II is due to the worse spectral sampling of energies above 4 Ryd.[8] For both H I and He II, the dispersion induced by RT in the photoionization rate values is significantly larger than that originating purely from numerical noise and, in the case of H I, it is increasingly so at larger values of Δ. Hence, this confirms that the effects we are finding are of physical origin and the corresponding fluctuations are a truly genuine byproduct of UVB filtering through cosmic density structures.

We have found so far that RT effects induce significant fluctuations in the metagalactic ionizing radiation; these could be effective in deviating the actual IGM ionization state from that inferred assuming a uniform ubiquitous UVB and hence should be accounted for in high-precision studies of the Lyα forest. However, performing full RT simulations is extremely expensive and prohibitive in maximum-likelihood analysis. The tight correlation between

[6] Note that these values are lower than those in Fig. 1, because here we consider only photons at the H I and He II ionization threshold.

[7] We use the OT simulation we have run to test the accuracy of the uniformity of the emission algorithm, with $N_{\rm p} = 3 \times 10^7$, having thus the same numerical resolution of the RT simulation.

[8] The number of photon packets emitted with energy above the He II threshold is roughly one order of magnitude smaller than $N_{\rm p}$.

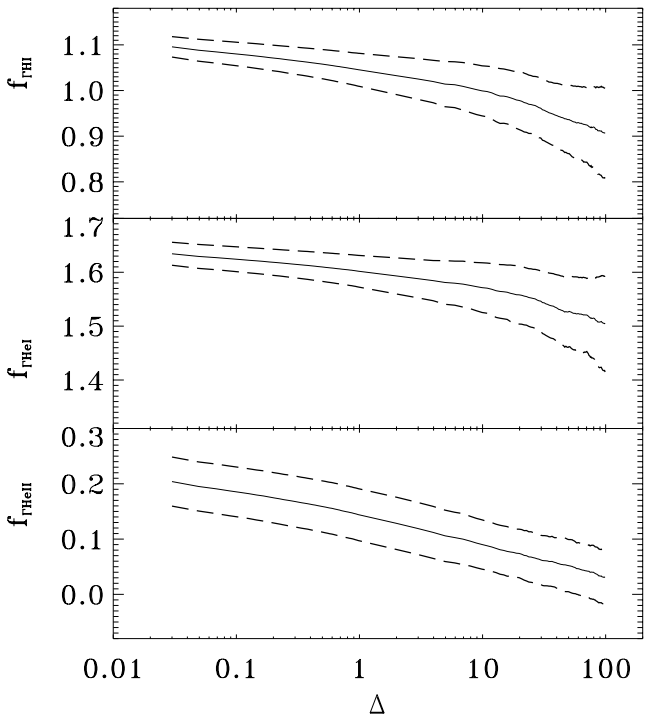

Figure 6. Photoionization rate correction factors (see equation 8) for H I (upper panel), He I (central panel) and He II (bottom panel), applicable at $z \approx 3$. The three panels show both the mean value (solid line) and the 1σ statistical error in each density bin.

fluctuations in the photoionization rate and overdensity can be used to correct the commonly adopted mean values derived in calculations (e.g. HM96; Fardal et al. 1998) carried out with one-dimensional RT calculations, under the assumption of photoionization equilibrium with a uniform UVB.

In order to cast our results in a form which could be useful for future studies, we have computed the photoionization rate correction factors from our RT simulations. These are defined as

$$\Gamma_i^{\rm RT}(\Delta) = f_{\Gamma_i}(\Delta)\Gamma_i^{\rm OT}(\Delta); \quad (8)$$

their mean values are plotted in Fig. 6 for H I, He I and He II (upper, central and bottom panels, respectively) along with the associated 1σ errors. These results are valid for $z \approx 3$. In a companion paper we will study the evolution with redshift of the UVB fluctuations. RT effects are generally more important in overdense regions, although the correction factors derived in the present study can be reliably used for $\Delta < 100$, a limit dictated by both mass resolution of the SPH simulation and shot noise associated with the limited number of photon packets. Differently from the case of H I, for which $\langle f_{\Gamma_{\rm HI}}\rangle \approx 0.98$ is close to unity, the mean values of the correction factors for He I and He II are $\langle f_{\Gamma_{\rm HeI}}\rangle \approx 1.56$ and $\langle f_{\Gamma_{\rm HeII}}\rangle \approx 0.2$ (averages are evaluated over the overdensity range $0.03 < \Delta < 100$). This reflects mean opacity differences among the three absorbers. In the OT approximation, the IGM opacity is higher in H I than in He I and, as a consequence, the UVB increase necessary to match the IGM H I Lyα opacity in RT simulations results in a higher mean $\Gamma_{\rm HeI}$. For the same reason, as the IGM OT opacity is by far higher in He II than in H I, $\langle\Gamma_{\rm HeII}\rangle$ is highly suppressed with respect to the OT value when RT effects are properly treated. Again, our results demonstrate that the contribution to the He II opacity of the diffuse IGM (as opposed to discrete absorbing systems) is relevant. The same arguments explain the steeper dependence of the He II correction factor from density and its larger dispersion.

It is worth making a few remarks concerning the correction factors. First, we remind that the adopted flux calibration (see Section 2) guarantees that the mean H I opacity in the RT simulation box corresponds to that at the photoionization equilibrium with the uniform UVB in the OT case. We have found that the mean values of $\Gamma_{\rm HI}$ in the two cases (RT and OT) are the same within a few per cent. Gnedin & Hamilton (2002) found a different result: in order to reproduce the same H I Lyα IGM transmissivity in their RT calculation, they required a 20 per cent higher volume-averaged H I photoionization rate with respect to the OT case. The reasons for the discrepancy are not clear, but it is probably due to the fact that while Gnedin & Hamilton (2002) account for RT during the reionization process (i.e. ionizing a neutral gas), here we redistribute the ionizing radiation accounting for RT effects in a pre-ionized gas. Meiksin & White (2003) also found that fluctuations required a boost in the radiation field, comparable to Gnedin & Hamilton; however, in a more recent investigation, they found that the boost is reduced to a few per cent at $z \lesssim 4$ when correlations in the radiation field due to RT were included (Meiksin & White 2004). This seems to suggest that the boost depends on the magnitude of the correlations in the radiation field.

It is furthermore interesting to note that $\Gamma_{\rm HI}$ can be fitted with a power law of the form $\Gamma_{\rm HI}(\Delta) = \Gamma^0_{\rm HI}\Delta^{-a_1}$ with $a_1 \simeq 0.022$. In the calculation of optical depth to the Lyα scattering given by (e.g. Weinberg 1999; McDonald & Miralda-Escudé 2001)

$$\tau = \tau_0 \frac{(1+z)^6\left(\Omega_{\rm b}h^2\right)^2}{T^{0.7}H(z)\Gamma_{-12,\rm HI}(z)}\Delta^{\beta}, \quad (9)$$

it is thus possible to account for UVB spatial fluctuations adopting a corrected index $\beta' = \beta + a_1$, i.e. $\tau \propto \Delta^{\beta'}/\Gamma^0_{-12,\rm HI}$, in a variation of the apparent IGM equation of state. Even though at $z \approx 3$ we found a negligible variation of β (only a few per cent), we expect the above effect to be important at higher redshifts.

Fig. 7 shows the PDF of the hydrogen photoionization rates resulting from our simulations (normalized to the volume-averaged mean value $\langle\Gamma_{\rm HI}\rangle$): the solid curve refers to the full RT simulation, whereas the dashed curve has been obtained from the OT simulation. The RT distribution is much wider than the OT distribution,

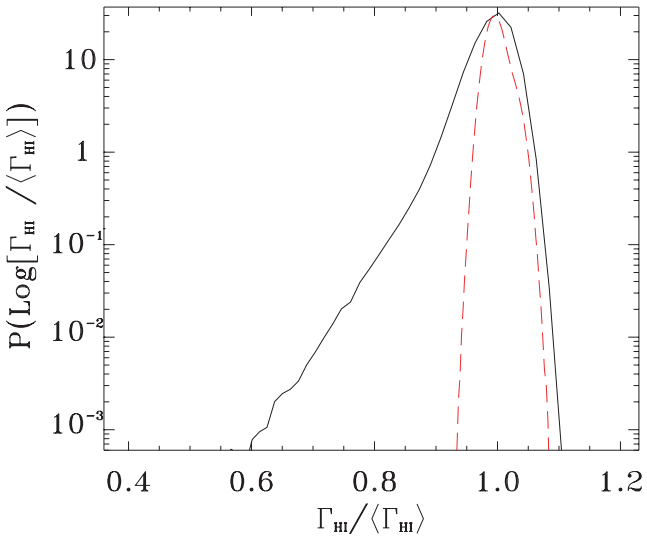

Figure 7. Comparison between the PDFs of the hydrogen photoionization rates, normalized with respect to the mean value, from full RT simulations (solid line) and OT simulations (dashed line).

showing an extended tail towards lower values of $\Gamma_{\rm H\,I}/\langle\Gamma_{\rm H\,I}\rangle$, which is caused by shadowing and shielding due to gaseous structures. There is also a slight increase of cells seeing an ionizing flux above the mean, occurring as a result of the flux amplitude redistribution. Further interesting aspects can be inferred comparing the UVB fluctuations produced by RT effects and those induced by the inhomogeneous distribution of rare quasars, assumed to be the dominant UVB sources, derived by Croft (2004) and shown in fig. 5 of that paper. Even in that case, the PDF of the ionizing flux appears to be asymmetric; however, the asymmetry is in the opposite direction. A similar result is obtained by Meiksin & White (2003), as shown in fig. 4 of that paper, where the effects of the source stochastic distribution in space are studied. In fact, fluctuations originating from the source inhomogeneous distribution are characterized by considerable power in the high flux tail ($\gtrsim$1.5 times the mean value), corresponding to the enhanced ionizing flux in the vicinity of the luminous ionizing sources. Hence, both RT and inhomogeneous distribution of ionizing sources contribute to broaden the radiation field distribution, basically increasing the power on opposite sides of the flux mean value. It is important to realize though that the spatial character of these fluctuations is very different. The signature of source inhomogeneities is seen on scales comparable to the typical separation of the sources, i.e. >100 Mpc for quasars. RT-induced fluctuations are instead found on a few (comoving) Mpc scales. To clarify this point, we have studied the spatial correlation of RT-induced UVB fluctuations, computing the $\delta\Gamma_i$ correlation function by using the following formula:

$$\mathcal{C}_i(\lambda) = \sum_{j=1}^{N_{\rm c}} \sum_{k\geqslant j}^{N_{\rm c}} \frac{\delta\Gamma_i(j)\delta\Gamma_i(k)}{N_\lambda}. \quad (10)$$

Here, the indices j and k span all the cells in the simulation grid, λ is the comoving separation between the jth and kth cells and N_λ is the number of pair cells whose distance is the range $[\lambda, \lambda + \Delta\lambda]$. We have similarly calculated a second correlation function, $\mathcal{C}_i^{\rm r}(\lambda)$, obtained from a random realization of $\delta\Gamma_i$, in the same volume and with the same mean as $\mathcal{C}_i(\lambda)$. The difference, $\bar{\mathcal{C}}_i(\lambda) = \mathcal{C}_i(\lambda) - \mathcal{C}_i^{\rm r}(\lambda)$ is plotted in Fig. 8 for H I and He II. The zero-point of these functions gives the characteristic correlation comoving length of the RT-induced fluctuations, which is found to be roughly 5.5 and 3.5 Mpc comoving for H I and He II, respectively. Although these results should be checked for convergency, by performing analogous simulations in larger volumes with the same resolution (Meiksin & White 2004), they seem to be plausible. The correlation scales we have found could be associated with the typical size/separation of filaments (i.e. mildly overdense regions) of the IGM, which are clearly identified in the maps presented in Fig. 2. These structures have optical depths $\gtrsim 0.1$ in both hydrogen and helium, and therefore can leave their imprint in the fluctuation field.

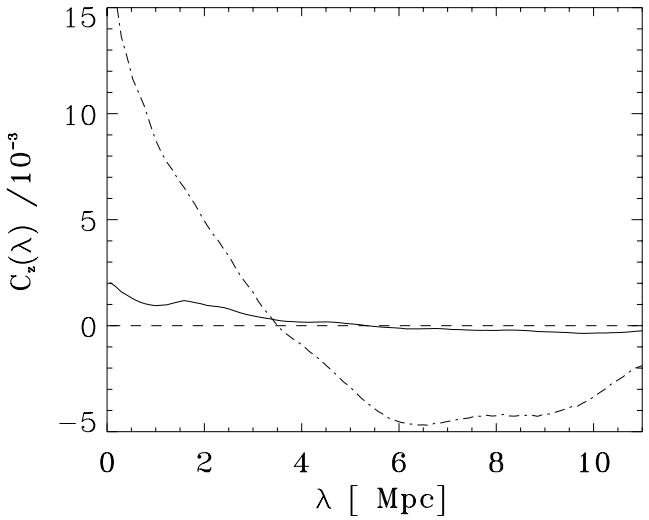

Figure 8. Correlation function (comoving scale) of photoionization rates for H I (solid line) and He II (dot-dashed line).

Meiksin & White (2003, 2004) have shown that the distribution of inhomogeneous sources (assumed to be QSOs) can produce correlations which are significant even on small scales. Both the RT-induced fluctuations and those originating from inhomogeneous source distribution should then be treated at once, in order to derive a correlation function which is reliable for the study of the pixel flux statistic in high-z QSO spectra.

3.2 He II/H I ratio fluctuations

The η parameter, defined as the ratio of He II to H I column density of an absorber in the Lyα forest, gives information on the intensity and on the spectral properties of the metagalactic ionizing radiation. Assuming photoionization equilibrium in highly ionized H/He gas, the following expression can be derived (Fardal et al. 1998):

$$\eta \equiv \frac{N_{\rm He\,II}}{N_{\rm H\,I}} = \frac{\alpha^{(A)}_{\rm He\,II}}{\alpha^{(A)}_{\rm H\,I}} \frac{n_{\rm He\,III}}{n_{\rm H\,II}} \frac{\Gamma_{\rm H\,I}}{\Gamma_{\rm He\,II}}. \quad (11)$$

Here, $\alpha^{(A)}_{\rm H\,I} = 2.51 \times 10^{-13} T_{4.3}^{-0.76} {\rm cm^3 s^{-1}}$ and $\alpha^{(A)}_{\rm He\,II} = 1.36 \times 10^{-12} T_{4.3}^{-0.70} {\rm cm^3 s^{-1}}$ are the case A recombination rate coefficients, appropriate in the low-density regime. We have derived the η parameter, for each cell of the numerical grid, from equation (11) with $n_{\rm He\,II}/n_{\rm H\,II}$ and $\Gamma_{\rm H\,I}/\Gamma_{\rm He\,II}$ taken from the RT simulation. The results are plotted in Fig. 9: the solid (dotted) line represents the mean η value derived in the RT (OT) simulation and the dashed curves are the 1σ rms deviations of the distribution.

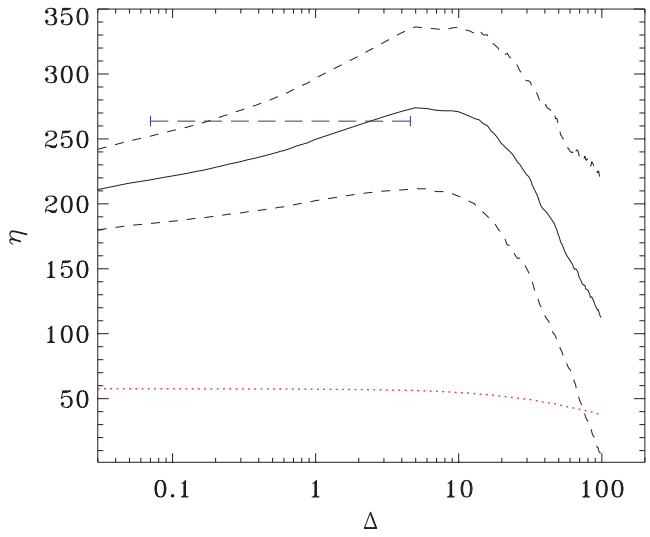

Figure 9. The parameter η is shown as a function of the overdensity Δ: the solid (dotted) line represents the mean η value from the RT (OT) simulation and the dashed curves correspond to 1σ rms deviation of the RT distribution. The long-dashed line shows the mean η value from Reimers et al. (2004) in the range of the observed densities (we exclude data points with $\Delta > 7$, as at higher densities the uncertainties on the η values inferred from observations become very high and metal line contamination is a problem).

In the OT case, as expected, η shows little dependence on Δ as a result of the fact that the three ratios in equation (11) are roughly constant. The ratio between the recombination coefficients slowly evolves with temperature, $\propto T_{4.3}^{0.06}$; the $\Gamma_{\rm H\,I}/\Gamma_{\rm He\,II}$ ratio does not vary by construction if the UVB is spatially uniform; finally, for $\Delta < 10$, the gas is fully ionized and thus $n_{\rm He\,II}/n_{\rm H\,II} \approx n_{\rm He}/n_{\rm H} = 0.785$ is roughly constant. At higher densities $n_{\rm He\,II}/n_{\rm H\,II}$ at the photoionization equilibrium starts to decrease because He II recombines faster than H II and $\Gamma_{\rm He\,II}/n_{\rm He}$ is roughly one order of magnitude lower than $\Gamma_{\rm H\,I}/n_{\rm H}$. The mean η value from our OT simulation is $\eta \approx 50$, consistent with the expected (from equation 11) value, $\eta \sim 0.43 \times \Gamma_{\rm H\,I}/\Gamma_{\rm He\,II} \approx 52$.

RT effects are crucial to determine the actual values of η in the IGM. This can be seen by comparing the previous results for the OT case with those from full RT calculations, shown in the same figure; the two cases differ from each other both in the mean value and in shape. The RT mean η value is larger than the OT value by about a factor of 4 because of the different amount of attenuation suffered by H I and He II ionizing radiation. As we have seen in Section 3, the He II ionizing flux is strongly suppressed with respect to the OT case, because even the most underdense voids in photoionization equilibrium with the UVB contain enough He II to remove photons with energies above 4 Ryd from the background radiation; the higher values we find for η in the RT simulation can be interpreted in terms of the ratios between the correction factors discussed in Section 3. The η parameter shows furthermore a strong dependence on overdensity: η slowly grows with density, reaches a maximum around $\Delta \approx 7$ and then rapidly declines to values which are still well in excess of the OT values. In fact, at low density $n_{\rm He\,II}/n_{\rm H\,II}$ is roughly constant, and density dependence is governed by $\Gamma_{\rm H\,I}/\Gamma_{\rm He\,II}$. This ratio increases with density as the Universe is more opaque in He II than in H I, as already discussed. When the density is high enough, $n_{\rm He\,II}/n_{\rm H\,II}$ decreases more rapidly than the growth of $\Gamma_{\rm H\,I}/\Gamma_{\rm He\,II}$, due both to the latter effect and to He III recombining faster than H II. This results in the inverted trend of the η dependence on Δ.

We compare our results from RT simulations with observational data by Reimers et al. (2004) in Fig. 9, using the relation $\Delta = 0.8\ N_{\rm H\,I,13}^{0.7}$ (Madau, Ferrara & Rees 2001). As the data released are still preliminary and could suffer from errors associated with the analysis technique (Fechner et al., private communication), we here consider the mean η value for $\Delta < 7$, as at higher densities the uncertainties on the η values inferred from observations become very high and metal line contamination is a problem. Although, it is important to point out that the dispersion in the data is substantial.

The comparison in Fig. 9 clearly shows that the mean η value from observations is inconsistent with the OT results, i.e. the expected value for the case of a spatially uniform UVB. The higher η measured value can be explained when accounting for the RT of the metagalactic ionizing radiation. Furthermore, at $\Delta > 7$, the RT simulation output predicts an η–Δ anticorrelation. This suggests that RT effects, such as shielding and shadowing, can explain the systematically lower η values observed in mildly/highly overdense absorption systems. According to our results, the lower values of η associated with high-density absorption systems do not arise, as previously thought, from the hardening of the UVB spectrum produced by the presence of local hard-spectrum sources. Instead, we find that the metagalactic ionizing flux is softer in filaments than in voids. Our preferred interpretation of the η trend seen in Fig. 9 is that the η–Δ anticorrelation is a direct consequence of the fact that in high-density regions $n_{\rm He\,II}$ increases much faster than $n_{\rm H\,I}$.

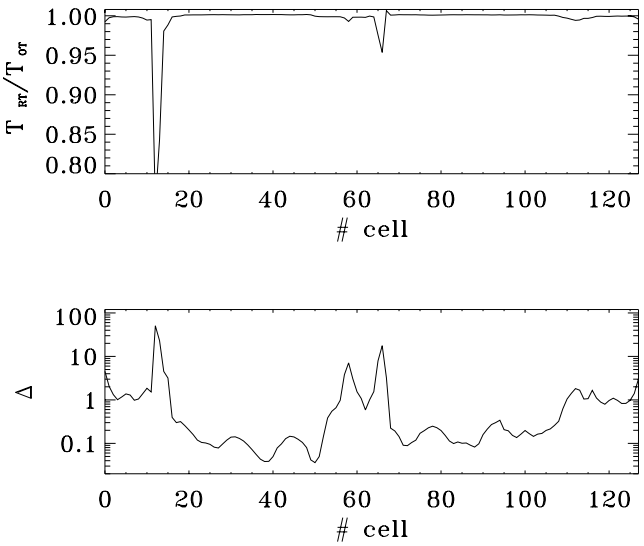

Figure 10. Upper panel: ratio between the temperature in the RT simulations, $T_{\rm RT}$, and the temperature estimated from the SPH simulation in the OT limit, $T_{\rm OT}$, along a typical light of sight. Lower panel: the overdensity, Δ, along the same line of sight.

3.3 Effects on the intergalactic medium temperature

Fluctuations in the photoionization rates could in principle affect the IGM temperature. In this subsection we attempt to quantify such an effect. The upper panel in Fig. 10 shows the ratio between the temperature in the RT simulations, $T_{\rm RT}$, and the initial temperature, $T_{\rm OT}$ (estimated in the SPH simulation in the OT limit), along a random line of sight; the lower panel shows the overdensity, Δ, along the same line of sight. The temperature ratio $T_{\rm RT}/T_{\rm OT}$ is significantly different from unity only in regions corresponding to high-density peaks, where the temperature shows deviations of the order of 1–2 per cent. The temperature in low-density regions is basically unchanged. This is not at odds with previous studies (Abel & Haehnelt 1999; Bolton et al. 2004) on the effect of RT on the temperature of the ionized gas, which indeed suggested that RT can be effective in boosting the IGM temperature by at least factor of 2 during the reionization process or in general when considering the photoionization of a neutral gas, with respect to the case in which the gas is instantaneously photoionized and photoheated by a uniform UVB. As discussed in Section 1, such a boost in temperature is due to the filtering of the ionizing radiation. The latter is significantly harder at the edge of the I-front, becoming harder as the I-front moves further from the source; this is due to the fact that the large cross-section, low-energy photons are selectively absorbed inside the H II region where they compensate for recombinations. The harder spectrum at the I-front yields a higher heating power with respect to analogous one provided by the unfiltered spectrum and, due to the long characteristic cooling times, the low-density IGM retains memory of the initial higher temperature phase. In the present study we focus on the transfer of ionizing radiation in an ionized IGM, and thus the above filtering process is not efficient due to the low IGM opacity. In order to account properly for RT effects on the IGM temperature, a full and consistent simulation of the reionization process including RT is necessary.

4 CONCLUSIONS

In this study we have analysed the effects of RT on the spatial and spectral properties of the ionizing metagalactic radiation at a

fixed redshift, $z = 3.27$. So far, this is the first attempt to study the properties of the UVB radiation including full three-dimensional RT calculations. Such an investigation is motivated by the increasing of observational evidence for a fluctuating UVB (Reimers et al. 2004; Shull et al. 2004). These observations reveal significant fluctuations on scales of a few comoving Mpc, which could hardly be originated from the inhomogeneous spatial distribution of ionizing sources, whose mean separation is $\approx 100\,h^{-1}$ Mpc for QSOs at $z \approx 3$.

We here neglect the UVB inhomogeneities arising from source clustering or non-uniform emissivity properties (which have been shown to be relevant only on large scales and at high redshift, i.e. $z > 4$), and focus on smaller scales. Our approach consists of performing RT simulations, applying CRASH to a cosmological density field exposed to an ionizing background characterized by a spatially constant emissivity. Such a radiation field, by interacting with the filaments of the cosmic web, is rapidly turned into a fluctuating one.

We have found that RT effects result in relevant fluctuations in the photoionization rates, whose structure is closely linked to the underlying density fluctuations. The UVB mean intensity, and thus its ionizing power, is progressively suppressed moving towards higher densities; such an effect is found to be more important for radiation above 4 Ryd, due the high He II opacity of the Universe. The ultimate physical nature of the decreasing trend of photoionization rates with density is a mixture of self-shielding and shadowing effects.

Interestingly, we found that the $\delta\Gamma_{\rm H\,I}$ dispersion increases towards higher Δ (from 8 per cent at $\Delta = 0.3$ to roughly 15 per cent at $\Delta = 3$), which is not the case for $\delta\Gamma_{\rm He}$. The differences in H I and He II photoionization rates originate from the fact that while the H I optical depth of the IGM is dominated by rare, overdense regions, the He II optical depth is non-negligible even in voids.

We further found that shielding in overdense regions ($\Delta \gtrsim 7$) from He II ionizing radiation produces a decreasing trend of the η parameter with overdensity; this trend has already emerged from observational data (Reimers et al. 2004; Shull et al. 2004). According to our results, the lower values of η associated with high-density absorption systems do not arise, as previously thought, from the hardening of the UVB spectrum produced by the presence of local hard-spectrum sources. Instead, RT simulations suggest that the η–Δ anticorrelation is a direct consequence of the fact that in high-density regions $n_{\rm He\,II}$ increases much faster than $n_{\rm H\,I}$. A stronger support for the presence of RT-induced UVB fluctuations comes from the comparison of the mean η value from Reimers et al. (2004) observations and our numerical results. We find in fact that the mean observed η value is too high to be consistent with a uniform UVB and that, accounting properly for the filtering of the ionizing radiation through the translucent IGM, it is possible to reconcile the observational data with theoretical expectations.

The results of the present study have several implications. In fact, the wealth of information derived from the Lyα forest has been so far extracted under the assumption of a uniform UVB, from both real and simulated data; the current results should thus be revised in order to account for the more realistic scenario of a fluctuating UVB. We give some examples. The matter power spectrum inferred from the observed/simulated transmissivity of the Lyα forest (Croft et al. 1999) provides direct information on the primordial Universe. UVB fluctuations could affect the power-spectrum shape derived in previous studies. Gnedin & Hamilton (2002) used RT simulations to study the effects of UVB fluctuations induced by the quasar inhomogeneous distribution on the matter power spectrum (however, they did not look directly at the RT effects on the spatial UVB fluctuations), not finding a significant variation. However, the question of whether small-scale fluctuations in the UVB could be relevant in determining the shape of the matter power spectrum needs further study.

The UVB fluctuations we have found could provide an alternative explanation, other than He II reionization occurring at $z \approx 3$, for the observed fluctuations in the η parameter as well as for those in the abundance ratio C IV/Si IV. As discussed in Section 1, it has been shown that current data are not inconsistent with a scenario in which He II is completely re-ionized as early as $z \sim 6$ by thermal radiation produced in collapsing structures (Miniati et al. 2004); the observed fluctuating C IV/Si IV abundance ratio and the He II patchy opacity could be then explained as direct consequences of UVB fluctuations arising from RT of the metagalactic ionizing radiation through the filamentary IGM.

Although in the present study we have carried out our analysis at $z \approx 3$, we can infer that the UVB fluctuations become more important towards higher redshift due to the increasing mean opacity of the IGM. In a future work we plan to investigate accurately the redshift evolution of UVB fluctuations.

Finally, it is worth reminding that we have neglected the possible contribution of local sources embedded in high-density regions to the ionizing radiation. The relative contribution of local sources embedded in quasar absorption-line systems, which are commonly identified as high-density peaks in the IGM, has been the subject of recent debate. Schaye (2004) argued that the contribution from local sources dominates the UV metagalactic radiation in these absorption systems, while Miralda-Escudé (2004) has come to the opposite conclusion, deriving an upper limit to the importance of local sources by a consequence of the surface brightness conservation. The problem seems still unsettled and it would be desirable to further investigate it via numerical RT simulations including both the UVB and the local source radiation.

ACKNOWLEDGMENTS

We acknowledge T. Choudhury and F. Haardt for enlightening discussions, and C. Fechner, J. Tumlinson and M. Shull for providing observational data. This work was partially supported by the Research and Training Network 'The Physics of the Intergalactic Medium' set up by the European Community under the contract HPRN-CT2000-00126 RG29185. The work has been completed at the Kavli Institute for Theoretical Physics Programme 'Galaxy–IGM Interactions', whose hospitality is warmly acknowledged.

REFERENCES

Abel T., Haehnelt M. G., 1999, ApJ, 502, L13
Bolton J. S., Meiksin A., White M., 2004, MNRAS, 348, L43
Bianchi S., Cristiani S., Kim T. S., 2001, A&A, 376, 1
Bruscoli M., Ferrara A., Marri S., Schneider R., Maselli A., Rollinde E., Aracil B., 2003, MNRAS, 343, L41
Croft R. A. C., 2004, ApJ, 610, 642
Croft R. A. C., Weinberg D. H., Pettini M., Hernquist L., Katz N., 1999, ApJ, 520, 1
Fan X., Narayanan V. K., Strauss M. S., White R. L., Becker R. H., Pentericci L., Rix H. W., 2002, ApJ, 123, 1247
Fardal M. A., Giroux M. L., Shull M. J., 1998, AJ, 115, 2206
Fechner C., Reimers D., 2004, in Sonneborn G., Andersson B.-G., Moos W., eds, ASP Conf. Ser., Astrophysics in the Far Ultraviolet: Five Years of Discoveries. Astron. Soc. Pac., San Francisco, in press (astro-ph/0410622)
Giallongo E., Fontana A., Madau P., 1997, MNRAS, 289, 629
Gnedin N. Y., Hamilton A. J. S., 2002, MNRAS, 334, 107
Haardt F., Madau P., 1996, ApJ, 461, 20 (HM96)

Kim T. S., Cristiani S., D'Odorico S., 2001, A&A, 373, 757
Kriss G. A. et al., 2001, Sci, 293, 1112
McDonald P., Miralda-Escudé J., 2001, ApJ, 549, 11
McDonald P., Seljak U., Cen R., Bode P., Ostriker J. P., 2005, MNRAS, 360, 1471
Madau P., Ferrara A., Rees M. J., 2001, ApJ, 555, 92
Marri S., White S. D. M., 2003, MNRAS, 345, 561
Maselli A., Ferrara A., Ciardi B., 2003, MNRAS, 345, 379 (MFC03)
Maselli A., Ferrara A., Bruscoli M., Marri S., Schneider R., 2004, MNRAS, 350, L21
Meiksin A., 2005, MNRAS, 356, 596
Meiksin A., White M., 2003, MNRAS, 342, 1205
Meiksin A., White M., 2004, MNRAS, 350, 1107
Miniati F., Ferrara A., White S. D. M., Bianchi S., 2004, MNRAS, 348, 964
Miralda-Escudé J., 2004, ApJ, 620, 91
Nakamoto T., Umemura M., Susa H., 2001, MNRAS, 321, 593
Navarro J. F., Frenk C. S., White S. M., 1996, ApJ, 462, 563
Reimers D., Fechner C., Kriss G., Shull M., Baade R., Moos W., Songaila A., Simcoe R., 2004, in Sonneborn G., Andersson B.-G., Moos W., eds, ASP Conf. Ser., Astrophysics in the Far Ultraviolet: Five Years of Discoveries. Astron. Soc. Pac., San Francisco, in press (astro-ph/0410588)
Schaye J., 2004, ApJ submitted (astro-ph/0409137)
Shull M. J., Roberts D., Giroux M. L., Penton S. V., Fardal M. A., 1999, AJ, 115, 2184
Shull M. J., Tumlinson J., Giroux M. L., Kriss G. A., Reimers D., 2004, ApJ, 600, 570
Sokasian A., Abel T., Hernquist L., 2003, MNRAS, 340, 473
Springel V., Yoshida N., White S. D. M., 2001, NewA, 6, 79
Steidel C. C., Pettini M., Adelberger K. L., 2001, ApJ, 546, 665
Telfer R. C., Zheng W., Kriss G. A., Davidsen A. F., 2002, ApJ, 565, 773
Weinberg D., 1999, in Banday A. J., Sheth R. K., da Costa L. N., eds, Evolution of Large-Scale Structure: From Recombination to Garching. European Southern Observatory, Garching, p. 346
Zuo L., 1992a, MNRAS, 258, 36
Zuo L., 1992b, MNRAS, 258, 45

This paper has been typeset from a TEX/LATEX file prepared by the author.